Algorithm to Generate a Discrete Element Specimen with Predefined Properties

H. K. Dang[1] and M. A. Meguid[2]

Abstract: The discrete element method is a powerful numerical tool in simulating the behavior of granular materials. It bridges the gap between continuum mechanics and physical modeling investigations. In spite of the significant achievements to date, some major problems are yet to be solved including the development of realistic large-scale models with initial conditions similar to those encountered in real problems. This paper introduces a computational method to generate a large-scale packing with predefined porosity and grain-size distribution in three-dimensional space based on a small initial sample packing. The developed method is implemented into an open-source computer code and used to generate specimens with known properties. The results showed that, under static condition, specimens generated using the proposed algorithm exhibited realistic behavior suitable for geotechnical applications. In addition, the controlled structure of the initial sample packing is successfully transferred to the final packing.

DOI: 10.1061/(ASCE)GM.1943-5622.0000028

CE Database subject headings: Discrete elements; Geotechnical engineering; Grain size; Porosity; Algorithms; Granular materials.

Author keywords: Discrete element method; Geotechnical engineering; Packing; Grain-size distribution; Porosity; Dynamic packing.

Introduction

Since the discrete element method was first introduced (Cundall and Strack 1979), it has been used extensively to investigate various engineering problems. One of the most important steps in a discrete element simulation is to generate a specimen (particle packing) in a form that represents realistic conditions. Several methods are currently available to randomly generate particle packing. These methods can be divided into three main categories: geometric; sedimentation; and dynamic methods. A brief overview of these methods is given below.

Geometric Methods

In these methods, a specimen is generated based on purely geometric calculations without simulating the dynamics of particle motion. Stoyan (1998) summarized different algorithms used to generate spheres simultaneously starting from a set of randomly located points. Evans (1993) developed the simple sequential inhibition model to place spheres sequentially and randomly in a given region. Cui and O'Sullivan (2003) suggested two-dimensional (2D) and three-dimensional (3D) assemblies of circular and spherical grains based on the triangulation approach. Although the 2D assemblies were successfully generated, the 3D packing encountered several performance problems. An improved method to generate a dense random packing in two dimensions was proposed by Feng et al. (2003) based on the advancing front approach. These methods, however, are generally applicable to 2D problems; the extension to 3D still needs further investigations.

Sedimentation Methods

Based on this approach, the translation of disks/spheres is determined based on purely geometric calculations, without analyzing the physical dynamics of the problems. Tory et al. (1968) developed the so-called sedimentation techniques. In this method, the required domain is filled up by placing disks/spheres following a user-defined size distribution into the domain and translating it downward until it collides with already existing disks/spheres in the system. Similar approaches have been employed by other researchers (Han et al. 2005; Fu and Dekelbab 2003).

Dynamic Methods

The advantage of the above methods is their computational efficiency. Packing process, however, involves various forces in addition to gravity (i.e., contact forces due to collision and friction among particles and interelement forces such as the van der Waals or electrostatic forces). These forces can affect the packing structure either individually or simultaneously depending on the packing condition. These phenomena are not considered in the purely geometric packing algorithms. A typical dynamic involves placing the required number of particles into a large domain whose walls are slowly moving inward until the required density is reached. Another possibility is to simulate gravitational deposi-

[1]Graduate Student, Dept. of Civil Engineering and Applied Mechanics, McGill Univ., 817 Sherbrooke St. West, Montreal, PQ H3A 2K6, Canada. E-mail: kien.dang@mail.mcgill.ca

[2]Assistant Professor, Dept. of Civil Engineering and Applied Mechanics, McGill Univ., 817 Sherbrooke St. West, Montreal, PQ H3A 2K6, Canada (corresponding author). E-mail: mohamed.meguid@mcgill.ca

Note. This manuscript was submitted on March 13, 2009; approved on August 7, 2009; published online on August 19, 2009. Discussion period open until September 1, 2010; separate discussions must be submitted for individual papers. This technical note is part of the ***International Journal of Geomechanics***, Vol. 10, No. 2, April 1, 2010. ©ASCE, ISSN 1532-3641/2010/2-85–91/$25.00.

tion where particles fall down freely into the domain, and their equilibrium position is established under the effect of gravity (Kong and Lannutti 2000). Liu et al. (1999) proposed a method to generate packing by imposing an assumed centripetal force on particles that are randomly generated in a spherical space. The above methods are considered to satisfactorily simulate the dynamics of forming a packing and produce realistic structural information, e.g., the radial distribution function (Jullien et al. 1996) and mean coordination number (Liu et al. 1999). However, they required a huge amount of calculation and therefore considered to be expensive and time consuming. In addition, the above methods do not address the generation of a packing with predefined porosity which is one of the important properties needed for geotechnical applications.

Input parameters for discrete element analysis are often derived by fitting data with the results from standard simulations using small assemblies of particles. Ng (2006) suggested that, under static conditions, such parameters (e.g., shear modulus, density, and damping) have negligible effects on the macroscopic behavior of the packing. The packing structure, on the other hand, is considered to be an important factor affecting the macroscopic behavior. The specimen used to simulate a given problem should, therefore, have the same structure as the sample used in the fitting process.

In this study, an algorithm combining the dynamic and geometric methods is proposed. Compared to the above methods, the proposed algorithm has the following advantages:

- The generated 3D packing has a realistic structure with a predefined grain-size distribution and porosity.
- Simulation time is reduced significantly by introducing a new geometric "flip" technique to generate a large-scale packing using an initial sample packing. The proposed flip technique can be applied to any particle shape.

Triaxial tests have also been conducted to demonstrate the structure conservation between the sample and the final packing. The developed algorithm was implemented into the Open Source computer code YADE (Kozicki and Donze 2008) using C++ programing. Although at the time of preparing this paper only spherical particles are available in the code, the algorithm can be applied to other particle shapes.

Governing Equations and Force Description

The contact forces are calculated based on the penalty method using the volume overlap of two interacting spheres.

Normal Forces

The normal forces are calculated as follows:

$$\mathbf{f}_{nci} = \mathbf{k}_n \boldsymbol{\delta}_n \tag{1}$$

where $\mathbf{f}_{nci}$=normal force at contact c of particle i; k_n=normal stiffness at the contact; $\boldsymbol{\delta}_n$=relative normal displacement between two particles; and $\mathbf{n}$=branch vector from the contact point to the particle center.

Shear Forces

The shear forces are calculated incrementally using (Hart et al. 1988)

$$\Delta \mathbf{f}_{sci} = \mathbf{k}_s \Delta \mathbf{u}_t \tag{2}$$

where $\Delta \mathbf{f}_{sci}$=incremental shear force; $\mathbf{k}_s$=tangential stiffness; and $\Delta \mathbf{u}_t$=incremental tangential displacement. The shear force is truncated if its absolute value is larger than the maximum value given by Mohr-Coulomb criterion

$$\mathbf{f}_{sci}^{\max} = |\mathbf{f}_{nci}| \times \tan \phi_i \tag{3}$$

where ϕ_i=internal friction coefficient.

The best fit method (Liao et al. 1997; Hentz et al. 2004) is employed in this study to establish the relationship between Young's modulus E, Poisson's ratio υ, and the dimensionless value of k_s/k_n

$$E = \frac{D_{\text{init}}^{a,b}}{S_{\text{init}}} k_n \frac{\beta + \gamma\beta + \gamma \dfrac{k_s}{k_n}}{\alpha + \gamma \dfrac{k_s}{k_n}} \tag{4}$$

$$\upsilon = \left(1 - \frac{k_s}{k_n}\right) \Big/ \left(\alpha + \frac{k_s}{k_n}\right) \tag{5}$$

where $D_{\text{init}}^{a,b}$=initial distance between the two interacting elements a and b; coefficients α, β, and γ=fitted values; and S_{init} = "interaction surface" given by

$$S_{init} = \pi[\min(R_a, R_b)]^2 \tag{6}$$

Stability Condition

The specimen is considered to be stable if the ratio of the unbalanced force to the total force is less than or equal to a predefined value. In this study, a value of 0.01% is used as indicated by Eq. (7) below

$$S_c = \frac{\Sigma |f_i|}{\Sigma |f_{nci}|} \leq 0.01\% \tag{7}$$

where f_i=resultant force on the body and f_{nci}=contact force.

Packing Generation Algorithm

The developed packing procedure consists of two phases: (1) a relatively small size initial packing is first generated with a predefined grain-size distribution and a desired porosity; (2) a final packing is then generated by assembling the small samples according to the geometric flip technique to maintain the same grain-size distribution and porosity. The above phases are discussed below.

Phase 1: Initial Packing

To generate an initial packing in a given space of known dimensions (b_x, b_y, and b_z) a number of particles are first generated without overlap in the predefined space. The particles are initially allowed to settle under gravity into a box with dimensions of $b_x \times b_z$ in plan. The height of the box is chosen to keep the rebounded particles inside [Fig. 1(a)]. Additional particles are generated after a predefined time interval (particle generation interval). Particle generation process is terminated when the total volume of the generated particles equals the total solid volume

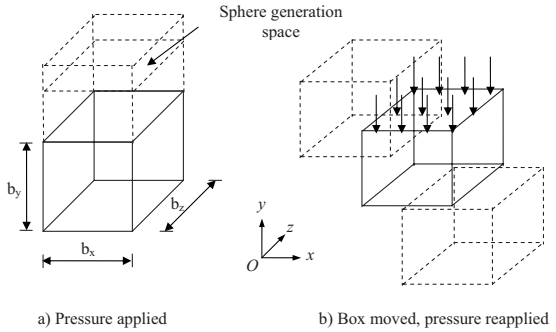

Fig. 1. Shaking procedures

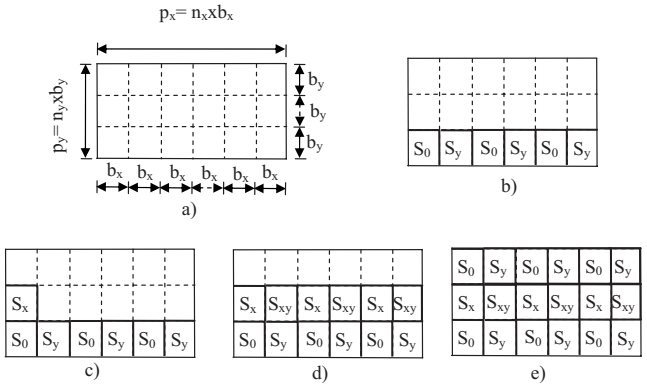

Fig. 2. Placing samples into the final domain

(V_s). The analysis continued until the packing reached the stability condition. The above procedure is called phase 0 in this study. The solid volume is calculated as

$$V_s = p \times b_x \times b_y \times b_z \tag{8}$$

where V_s=volume of the particles; p=target porosity; and b_x, b_y, and b_z=packing dimensions in the x, y, and z directions, respectively.

Generating Spheres with a Predefined Grain-Size Distribution

In digital elevation model (DEM) simulation, it is rather convenient to generate a packing that corresponds to a given grain-size distribution by controlling the particle number than the particle weight. Thus the results of the sieve analysis that is usually expresses as a percentage passing by weight through a series of sieves should be converted to a percentage passing by number of spheres. A generator is used to produce a pseudorandom number between 0 and 1. For spherical particles, the radius of particle i is calculated using the following equation to generate a population of particles consistent with the sieve analysis result:

$$r_i = [D_1 + (RAN_i \times 100 - P_1) \times (D_2 - D_1)/(P_2 - P_1)]/2 \tag{9}$$

where r_i=radius of particle i and P_1 and P_2=total number of grains (%) calculated from the percentage volume passing through sieves S_1 and S_2, respectively. D_1 and D_2=diameters of sieves S_1 and S_2, respectively. RAN_i=ith random number generated for particle i such that $RAN_i \times 100 \geq P_1$ and $RAN_i \times 100 < P_2$. Sieves S_1 and S_2 are determined by comparing RAN_i with the results of the sieve analysis. The radius of the generated spheres (r_i) is related to the random number generator and may, therefore, differ from the target grain-size distribution, depending on the random number generator.

Adjusting the Initial Packing to Obtain a Target Porosity

The initial packing generated using the above procedure is considered to produce a loose structure. Thus, it is usually compacted to reach a realistic porosity. This is not generally feasible to achieve if only a static pressure (σ_{iso}) is applied over the particles. Therefore, a technique that involves applying a combination of shaking and vertical compression is adopted in this study as described below.

For each time step, all the walls are assigned a movement in the x-, y-, and z-directions. The magnitudes of the movements are calculated by multiplying the given velocity and the time step. The additional movement of the top wall is calculated based on the applied force acting in the normal (y) direction

$$d_{wall} = (F - F_{cwall})/k_{wall} \tag{10}$$

where d_{wall}=additional wall movement; F=force applied to the wall; F_{cwall} and k_{wall}=sum of forces and normal stiffnesses over the wall contacts, respectively.

The porosity of the packing is monitored by calculating the average packing height and the process is terminated when the required height (b_y) is obtained. Since the packing height is measured during the shaking process, the walls stop temporality for a period of time so that the particles can settle down. At the same time the external force at the top wall is released. The walls are then allowed to move with the same velocities but in the opposite directions together with the activation of the external force on the top wall [Fig. 1(b)]. After the required height is reached, the DEM simulation continued until the stability condition is satisfied.

Phase 2: Final Packing

To overcome the large amount of computations associated with the dynamic packing method, a geometric method called the flip technique is proposed. The algorithm is three dimensions in nature; however, for the sake of simplicity, it is presented here in two dimensions.

To generate a final packing with dimensions of p_x and p_y in the x- and y-directions, respectively, the packing space is divided into $n_x \times n_y$ domains [Fig. 2(a)]. An initial packing S_0 ($b_x \times b_y$) is first generated using the technique described in "Adjusting the Initial Packing to Obtain a Target Porosity" section and then cloned repeatedly to obtain a final packing with similar properties (grain-size distribution, porosity, mean coordination number, and fabric tensors). As the structure of the packing is mainly supported by the force chains, it is necessary to maintain the force chains in each initial packing after the assembly. This is achieved by flipping the initial packing such that all particles (initially in contact with the walls) become in contact with other particles in the final packing. As shown in Fig. 3, sample S_x is obtained by flipping S_0 around the x axis. Similarly, S_y is obtained by flipping S_0 around the y axis. Finally, S_{xy} is obtained by flipping S_x around the y axis (or flipping S_y around the x axis).

Samples S_0, S_x, S_y, and S_{xy} are then placed into the space of the final packing as follows:

- The initial packing is placed into the lower left corner of the domain. Sample S_y is then placed to the right of sample S_0 and

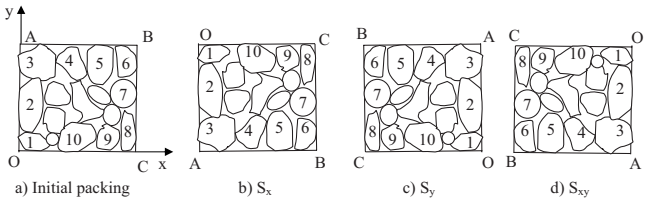

Fig. 3. Flipping scheme of the initial packing

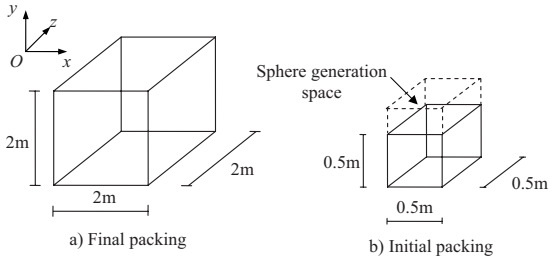

Fig. 5. Sketch of the packing dimensions

the process is repeated until the bottom row is completed [Fig. 2(b)].

- The sample to be placed on top of sample S_0 should have particles 3, 4, 5, and 6 placed in the same order as the sample S_0. Consequently, sample S_x is chosen [Fig. 2(c)].
- Similarly, sample S_{xy} is chosen to be placed next to sample S_x. Note that particles at the bottom of sample S_{xy} (particles 6, 5, 4, and 3) are also in contact with identical particles at the top of sample S_y. The procedure is repeated until the second row is completed [Fig. 2(d)]. The assembly of the samples in the final packing is shown in Fig. 2(e).

After filling up the final domain, the simulation continued until the final packing satisfies the stability condition. It should be noted that the normal forces acting on particles next to the wall remain the same after the small sample is flipped. For the sake of simplicity, the discussions will be focused on the interaction of spherical particles in this study. The extension to other particle shapes can be carried following the same procedure. Considering the interaction between two spheres as shown in Fig. 4(a), the normal penetration in Eq. (1) can be calculated as

$$\delta_n = 0.5(R_1 + R_2 - O_1O_2) \tag{11}$$

where δ_n=normal penetration; R_1 and R_2=radii of spheres 1 and 2, respectively; and O_1O_2=distance between the centers of the two spheres.

The normal penetration depth of the interaction between a sphere and a wall [Fig. 4(b)] is calculated as

$$\delta_n = R_1 - O_1W \tag{12}$$

where W=projection of the sphere center to the wall. As the sphere is generated using the flip technique [Fig. 4(c)], the distance between the centers of the two spheres is equal to $2O_1W$. Substituting into Eq. (11), we obtain

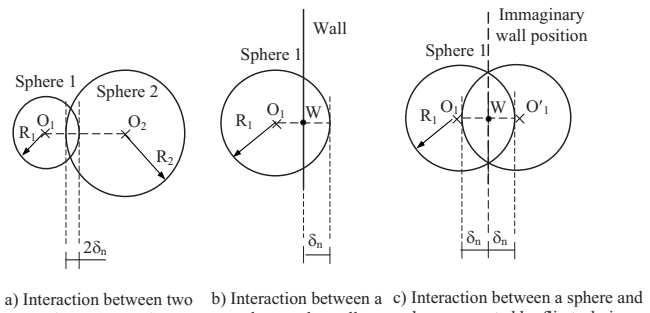

Fig. 4. Schematic of sphere interactions

$$\delta_n = 0.5(R_1 + R_1 - O_1O_1') = 0.5(2R_1 - 2O_1W) = R_1 - O_1W \tag{13}$$

By comparing Eqs. (12) and (13), it can be concluded that the penetration depth used in Eq. (1) is identical for the interactions between a sphere and a wall (before flipping) and between two spheres (after flipping). This leads to the conservation of forces acting on the spheres at the boundaries and, therefore, the structure of the initial packing is preserved in final packing.

Numerical Simulation

Packing Generation

To validate the proposed algorithm, simulations were carried out to fill up a final packing (2 m×2 m×2 m) as shown in Fig. 5(a). The material properties used in the simulation are given in Table 1. The target grain-size distribution is given in Table 2. The target porosity is chosen to be 0.38 which is typical for sands. The final packing is generated from the cubical shaped initial packings (S_0) with the dimensions of 0.5-m height, 0.5-m width, and 0.5-m depth as illustrated in Fig. 5(b).

Table 1. Material Properties

Parameter	Value
Particle density (kg/m^3)	2600
Young's modulus (Pa)	15×10^6
Poisson's ratio	0.5
Friction (deg)	18
The Box-Poisson ratio	0.2
Box's friction (deg)	0
Force damping coefficient	0.2
Moment damping coefficient	0.2

Table 2. Grain-Size Distribution

Sieve diameter (mm)	Input grain-size distribution		Result grain-size distribution	
	% passing (weight)	% passing (number)	% passing (number)	% passing (weight)
10	0	0	0	0
20	2	31.47	34.47	2.72
50	50	90.93	94.40	62.77
80	95	99.64	99.8	94.46
100	100	100	100	100

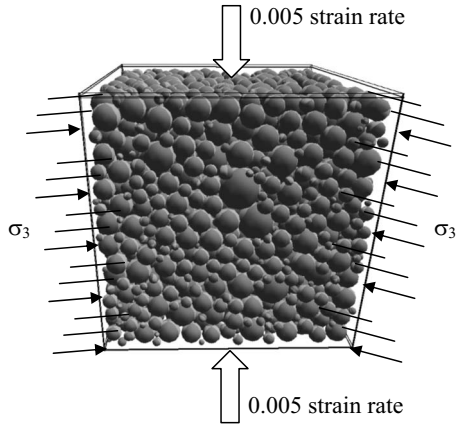

Fig. 6. Snapshot of the triaxial test simulation (3,629 particles)

Triaxial Tests

To calibrate the behavior of the initial (S_0) and final packings, triaxial tests are carried out using the obtained packing structures. In these simulations, boundaries are moved at a strain rate of 0.01. This value is chosen so that the unbalanced force is significantly small compared to the contact force; i.e., the system is always close to equilibrium. The sample is first compressed isotropically using an all around confining pressure. Two different values of confining stresses are adopted, namely, 50 and 100 kPa, in the analysis. After the stability condition is reached, additional 0.01 strain rate is applied to the top wall while the lateral confining pressure is kept constant. The reaction stresses are then calculated from the contact forces acting on the walls. During the simulation, gravity field is set to zero. The configuration of the specimen used in the triaxial test is shown in Fig. 6.

Results and Discussion

The general characteristics of the generated packing are summarized in Table 3. Phase 0 represents the packing obtained after the pouring procedure only. It can be seen that the required properties have been generally satisfied in the final packing. The obtained packing porosity has a value of 0.377, while the target porosity is 0.38. The grain-size distribution obtained (Table 2) is slightly different from the input one as predicted when a random number generator is used. It is, however, desired to demonstrate the randomness of the packing algorithm. The simulation time for the initial sample packing was about 1 h and 45 min, whereas the total time for the final packing (which depends on the packing size) was approximately 90 h; most of it has been mostly used to satisfy the stability condition. It should be noted that generating a packing of similar dimensions to the final packing shown in Fig. 5(a) without using the proposed flip technique would take up to 1560 h (using the same computer) to obtain the required properties (e.g., grain-size distribution and porosity).

Table 3. General Characteristics of the Packing

Packing properties		Phase 0	Phase 1	Phase 2
Height (m)		0.539	0.499	1.99
Total number of particles		3,629	3,629	232,256
Porosity		0.43	0.379	0.377
Mean coordination number		6.47	5.52	5.514
Simulation time (s)		4,544	6,709	356,173
Fabric tensor components	xx	0.339	0.339	0.3385
	yy	0.32	0.321	0.322
	zz	0.34	0.339	0.3385
	xy	-1×10^{-5}	0.002	1.18×10^{-5}
	xz	-5.33×10^{-5}	-0.001	-1.66×10^{-5}
	yz	-5×10^{-4}	-0.002	1.15×10^{-5}

Note: Phase 0 means the packing obtained from the sedimentation.

Coordination Number

As shown in Table 3, the mean coordination numbers for phase 0 (after the completion of the particle pouring step) have a value of 6.47. This value is generally in good agreement with the results of Pinson et al. (1998) who investigated the packing properties prepared using the pouring technique. They concluded that the mean coordination number oscillates around a constant value of 6.29 in average, independent of the particle size distribution.

An interesting observation has been made in the above simulations related to the changes in the mean coordination number with the change in the packing density. When the packing is modified to obtain the required porosity, the resulted packing no longer has the same structure as the one obtained using the conventional pouring technique. A decrease in the mean coordination number, from 6.47 in phase 0 to 5.52 in phase 1, was observed as shown in Table 3. This decrease in the mean coordination number was not expected since a denser packing usually has a higher mean coordination number. However, since the packing in phase 1 is generated using a different method, the above values are considered to be irrelevant. It should also be noted that, based on the analysis results, a value of 4 for the mean coordination number was sufficient for the packing to be stable.

Fabric Tensor (F_{ij})

In soil mechanics, the term fabric is used to refer to the arrangement of particles, particle groups, and pore spaces. Quantitative measures of fabric are usually considered to investigate the characteristics of a given soil system (e.g., degree of homogeneity and isotropy). In DEM simulations fabric can be quantified using the fabric tensor (Luding 2004). The contact fabric tensor (second rank) can be expressed as

$$F_{ij} = \frac{1}{N_c}\sum_{N_c} n_i n_j \tag{14}$$

where N_c=number of contacts and n_i and n_j=contact normals in the i- and j-directions, respectively.

Table 3 shows the fabric tensor components for the packing in phase 0, phase 1, and phase 2. The fabric tensor components in the x- and z- (horizontal) directions are about the same, whereas the component in the y- (vertical) direction is slightly smaller due to the presence of gravity. By comparing the fabric tensor components in the three different phases, it can be seen that the magnitude of the fabric tensor remains almost unchanged. Since the fabric tensor is strongly related to the stiffness and volumetric behavior of the assemblies (Luding 2004), the stress-strain behavior is expected to also remain unchanged from the initial sample to the final packing. The stress-strain behavior will be further discussed in "Stress Strain Behavior" section.

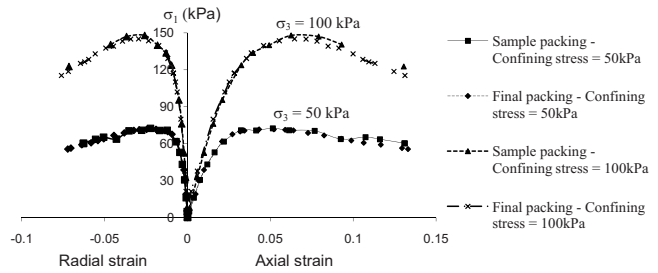

Fig. 7. Triaxial test results

Stress Strain Behavior

Fig. 7 illustrates the stress-strain behavior of the sample and final packing under confining stresses of 50 and 100 kPa, respectively. The initial stiffness generally increased with increasing the confining stress. The peak strengths are observed to be identical for both the sample and final packing regardless of the applied confining stresses. The stress-strain behavior shows also a postpeak softening behavior for all examined structures such that axial and radial strains increased with the decrease of the axial stress. In general, the stress-strain behavior of the two packing systems is almost identical for the examined range of confining stresses. This is attributed to the insignificant changes to the sample packing as compared to the final packing structures (coordination numbers, porosities, and fabric tensors).

Stress Distribution

To investigate the stress distribution in the final packing, the macroscopic stress tensor can be determined using (Matuttis et al. 2000)

$$\sigma_{ij} = \frac{1}{V} \sum_{p \in V} \sum_{c=1}^{c} l_i^c f_i^c \tag{15}$$

where V=representative "averaging" volume; f_i^c=force acting at contact; l_i^c=branch vector from the particle center to the contact point c; and indices i and j indicate the Cartesian coordinates.

To examine the geostatic stress distribution inside the final packing, stresses are averaged over representing volumes. The calculated stresses S_{xx}, S_{yy}, and S_{zz} in the x-, y-, and z-directions are shown in Fig. 8. The stress distribution generally satisfied the expected geostatic stress distribution except at as some local areas around the corners of the initial samples. This is attributed to the remaining wall effect in the samples before the assembly process.

To quantify the stress distribution and compare it to the theoretical values, the stresses are averaged along a plane normal to the y axis and the results are presented in Fig. 8 along with the expected theoretical values for comparison purpose. The theoretical lateral pressure is determined by multiplying the vertical stress by the lateral earth pressure coefficient at rest (K_0) often used in conventional soil mechanics and described by

$$K_0 = 1 - \sin \phi' \tag{16}$$

where ϕ'=effective friction angle.

By fitting the simulation data of the sample packings with Mohr-Coulomb failure criterion, a friction angle of 23.7° is obtained and used in Eq. (16) to determine the K_0 value. It can bee seen that both the vertical and lateral stresses obtained based on the proposed algorithm are in good agreement with the theoretical values as illustrated in Fig. 8.

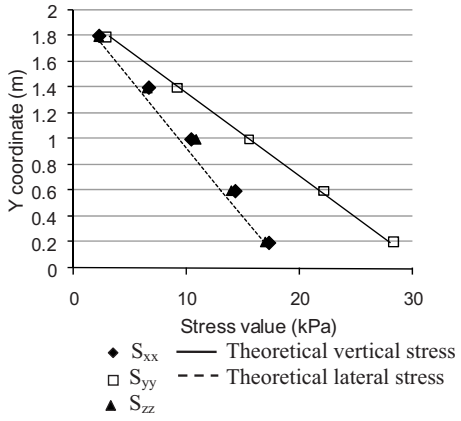

Fig. 8. Stress distribution profile

Summary and Conclusions

An algorithm to generate particle packing with predefined grain-size distribution and porosity was proposed. Numerical simulations were carried out to evaluate the performance of the proposed algorithm. Packing is generated by assembling small size samples, which have been subjected to a densification process, using the proposed flip technique. This procedure has proven to be successful in maintaining the structure of the generated samples in the final packing and produced realistic properties and stress distribution within the final packing. The sample packing can generally be adjusted to have a specific structure and then a simulation can be carried out on the assembled large-scale final packing. It should be noted that even though the developed algorithm has resulted in significant decrease in computation time, it is only applicable to generate boxlike shaped packing systems.

Acknowledgments

This research was supported by a research grant from the Natural Sciences and Engineering Research Council of Canada (NSERC). The financial support provided by McGill Engineering Doctoral Award (MEDA) to the first writer is greatly appreciated.

Notation

The following symbols are used in this paper:

b_x, b_y, and b_z = packing dimensions;
$D_{\text{init}}^{a,b}$ = initial distance between the two interacting elements a and b;
D_1 and D_2 = diameters of sieves;
d_{wall} = additional movement;
F = force applied to the wall;
F_{cwall} and k_{wall} = sum of forces and normal stiffnesses;
f_i = resultant force;
f_i^c = force acting at contact;
$\mathbf{f}_{nci}$ = normal force at contact c of particle i;
k_n = normal stiffness;

$\mathbf{k}_s$ = tangential stiffness;
l_i^c = branch vector from the particle center to the contact point c;
N_c = number of contacts;
$\mathbf{n}$ = branch vector from the contact point to the particle center;
n_i and n_j = contact normals in the i- and j-directions;
P_1 and P_2 = total number of grains;
RAN_i = ith random number;
S_c = stability value;
S_{init} = interaction surface;
V = representative averaging volume;
V_s = volume of particles;
α, β, and γ = fitted values;
$\Delta\mathbf{f}_{sci}$ = incremental shear force;
$\Delta\mathbf{u}_t$ = incremental tangential displacement;
$\boldsymbol{\delta}_n$ = relative normal displacement; and
ϕ_i = internal friction coefficient.

References

Cui, L., and O'Sullivan, C. (2003). "Analysis of a triangulation based approach for specimen generation for discrete element simulations." *Granular Matter*, 5(3), 135–145.

Cundall, P. A. and Strack, O. D. L. (1979). "A discrete numerical model for granular assemblies." *Geotechnique*, 29(1), 47–65.

Evans, J. W. (1993). "Random and cooperative sequential adsorption." *Rev. Mod. Phys.*, 65, 1281–1329.

Feng, Y. T., Han, K., and Owen, D. R. J. (2003). "Filling domains with disks: An advancing front approach." *Int. J. Numer. Methods Eng.*, 56(5), 699–713.

Fu, G., and Dekelbab, W. (2003). "3-D random packing of polydisperse particles and concrete aggregate grading." *Powder Technol.*, 133, 147–155.

Han, K., Feng, Y. T., and Owen, D. R. J. (2005). "Sphere packing with a geometric based compression algorithm." *Powder Technol.*, 155(1), 33–41.

Hart, R., Cundall, P. A., and Lemos, J. (1988). "Formulation of a three-dimensional distinct element model—Part II. Mechanical calculations for motion and interaction of a system composed of many polyhedral blocks." *Int. J. Rock Mech. Min. Sci. Geomech. Abstr.*, 25(3), 117–125.

Hentz, S., Daudeville, L., and Donze, F. V. (2004). "Identification and validation of a discrete element model for concrete." *J. Eng. Mech.*, 130(6), 709–719.

Jullien, R., Jund, P., Caprion, D., and Quitmann, D. (1996). "Computer investigation of long-range correlations and local order in random packings of spheres." *Phys. Rev. E*, 54(6), 6035–6041.

Kong, C. M., and Lannutti, J. J. (2000). "Effect of agglomerate size distribution on loose packing fraction." *J. Am. Ceram. Soc.*, 83(9), 2183–2188.

Kozicki, J., and Donze, V. F. (2009). "YADE-OPEN DEM: An open-source software using a discrete element method to simulate granular material." *Engineering Computations: Int. J. for Computer-Aided Engineering*, 26(7), 786–805.

Liao, C. L., Chang, T. P., Young, D. H., and Chang, C. S. (1997). "Stress-strain relationship for granular materials based on the hypothesis of best fit." *Int. J. Solids Struct.*, 34(31&32), 4087–4100.

Liu, L. F., Zhang, Z. B., and Yu, A. B. (1999). "Dynamic simulation of the centripetal packing of mono-sized spheres." *Physica A*, 268(3&4), 433–453.

Luding, S. (2004). "Micro-macro transition for anisotropic, frictional granular packings." *Int. J. Solids Struct.*, 41, 5821–5836.

Matuttis, H. G., Luding, S., and Herrmann, H. J. (2000). "Discrete element simulations of dense packings and heaps made of spherical and non-spherical particles." *Powder Technol.*, 109(1–3), 278–292.

Ng, T.-T. (2006). "Input parameters of discrete element methods." *J. Eng. Mech.*, 132(7), 723–729.

Pinson, D., Zou, R. P., Yu, A. B., Zulli, P., and McCarthy, M. J. (1998). "Coordination number of binary mixtures of spheres." *J. Phys. D: Appl. Phys.*, 31, 457–462.

Stoyan, D. (1998). "Random sets: Models and statistics." *Int. Statist. Rev.*, 66(1), 1–27.

Tory, E. M., Corchane, N. A., and Waddell, S. R. (1968). "Random sets: Models and statistics." *Nature (London)*, 220, 1023–1024.